Journal of South American Earth Sciences 64 (2015) 339–350

Contents lists available at ScienceDirect

Journal of South American Earth Sciences

journal homepage: www.elsevier.com/locate/jsames

Active deformation in the northern Sierra de Valle Fértil, Sierras Pampeanas, Argentina

Gustavo Ortiz [a, *], Patricia Alvarado [a], Julie C. Fosdick [b], Laura Perucca [a], Mauro Saez [a], Agostina Venerdini [a]

[a] Centro de Investigaciones de la Geósfera y la Biósfera (CIGEOBIO), Facultad de Ciencias Exactas, Físicas y Naturales, Universidad Nacional de San Juan – Consejo Nacional de Investigaciones Científicas y Técnicas (CONICET), Meglioli 1160 S, Rivadavia, 5406, San Juan, Argentina
[b] Department of Geological Sciences, Indiana University, 1001 East Tenth Street, Bloomington, IN 47405, USA

ARTICLE INFO

Article history:
Received 21 December 2014
Received in revised form
12 August 2015
Accepted 29 August 2015
Available online 1 September 2015

Keywords:
Sierra de Valle Fértil
Basement-cored uplift
Thermochronology
Flat-slab subduction

ABSTRACT

The Western Sierras Pampeanas region in the San Juan Province is characterized by thick-skinned deformation with approximately N–S trending ranges of average heights of 2500 m and a high frequency occurrence of seismic activity. Its location to the east of the mainly thin-skinned tectonics of the Argentine Precordillera fold-and-thrust belt suggests that at 30°S, deformation is concentrated in a narrow zone involving these two morphostructural units. In this paper, we present new apatite (U–Th)/He results (AHe) across the northern part of the Sierra de Valle Fértil (around 30°S) and analyze them in a framework of thermochronologic available datasets. We found Pliocene AHe results for Carboniferous and Triassic strata in the northern Sierra de Valle Fértil consistent with the hypothesis of recent cooling and inferred erosional denudation concentrated along the northern end of this mountain range. Our analysis shows that this northern region may have evolved under different conditions than the central part of the Sierra de Valle Fértil. Previous studies have observed AHe ages consistent with Permian through Cretaceous cooling, indicating the middle part of the Sierra de Valle Fértil remained near surface before the Pampean slab subduction flattening process. Those studies also obtained ~5 My cooling ages in the southern part of the Sierra de Valle Fértil, which are similar to our results in the northern end of the range. Taken together, these results suggest a pattern of young deformation in the northern and southern low elevation ends of the Sierra de Valle Fértil consistent with regions of high seismic activity, and Quaternary active faulting along the western-bounding thrust fault of the Sierra de Valle Fértil.

1. Introduction

Basement-involved deformation is an unusual feature in retro-arc foreland regions of orogenic belts, and for this reason comparisons between ancient and modern basement-cored uplifts (like the Northamerican Laramide Rocky Mountains versus Argentinean Sierras Pampeanas) have been performed in order to better understand the mountain building processes responsible for this deformation (Jordan and Allmendinger, 1986; Ramos, 2000). Many years of investigations in worldwide tectonics has led scientists to propose flat-slab subduction as the mechanism that drives strain into the foreland, and hence deformation. This link between the timing of slab shallowing and the record of orogenic exhumation in the Argentine broken-foreland basin has been well documented in a continuous study of its structural, magmatic, tectonic and sedimentary history (Jordan et al., 1983a,b; Strecker et al., 1989; Allmendinger et al., 1990; Kay et al., 1991; Ramos et al., 2002). In light of the fact that thermochronology may place quantitative constraints on the timing and magnitude of rock exhumation, relatively few low-temperature thermochronology studies have been conducted in the Argentinean Sierras Pampeanas. It is worth to note that the Sierra de Valle Fértil (SVF) lying above the flat-slab subduction of the Nazca Plate offers an ideal scenario to test signals of uplift/faulting and exhumation.

The aim of this paper is to identify and characterize the style of deformation in the northern SVF, which is part of the western

* Corresponding author. CIGEOBIO-Grupo de Sismotectónica, Facultad de Ciencias Exactas, Físicas y Naturales, Universidad Nacional de San Juan, Meglioli 1160 Sur, Rivadavia, 5406, San Juan, Argentina.
E-mail addresses: gfortiz@unsj-cuim.edu.ar (G. Ortiz), alvarado@unsj-cuim.edu.ar (P. Alvarado), jfosdick@indiana.edu (J.C. Fosdick), lperucca@unsj-cuim.edu.ar (L. Perucca), msaez@unsj-cuim.edu.ar (M. Saez), agostina.venerdini@unsj-cuim.edu.ar (A. Venerdini).

http://dx.doi.org/10.1016/j.jsames.2015.08.015
0895-9811/

Sierras Pampeanas (Fig. 1) combining new low-temperature thermochronology data, neotectonic and seismic activity evidences. Constraints on the timing and magnitude of exhumation compared to current deformation data in this region can provide insights about mechanisms of basement-cored uplifts into the Andean foreland, which are typically exposed in the flat slab subduction region of Argentina.

Recent investigations of exhumation patterns in the Sierras Pampeanas using low-temperature thermochronological techniques depict overall low (<2–3 km) magnitudes of exhumation, most of which has been attributed to pre-Cenozoic events and to a lesser degree, Cenozoic exhumation (Coughlin et al., 1998; Löbens et al., 2011, 2013; Bense et al., 2013). These studies used zircon and apatite (U–Th-Sm)/He (ZHe and AHe, respectively), zircon and apatite fission track (ZFT and AFT, respectively) thermochronology and K–Ar dating of fault gouge in order to better estimate the timing and rates of exhumation and inferred uplift of this wide morphotectonic area in central Argentina. Previous results from Coughlin et al. (1998) show two pre-Andean cooling events during late Paleozoic and late Mesozoic related to a Permian–Triassic flat-slab subduction and Mesozoic rifting events, respectively. This late Paleozoic flat-slab subduction is supported by evidence of an eastward propagation of calk-alcaline magmatism followed by extensional collapse of previous orogenic building (Ramos, 1994; Martinez et al., 2006). In addition, two phases of Andean events were recognized by Coughlin et al. (1998): an Early Miocene heating event corresponding to foreland basin sedimentation loading and a Miocene-Pliocene exhumation starting at ca. 10 Ma which involved some Precordillera front uplift and sediment recycling (Jordan et al., 1983a,b; Coughlin et al., 1998; Fosdick and Carrapa, 2012). Dávila and Carter (2013) performed studies at the base of the ~10 km thick exposed Cenozoic deposits of the Vinchina Basin, showing unreset pre-Cenozoic thermochronology data, which remain inconsistently. According to their AFT data these pre-Cenozoic patterns of deformation were related to burial heating followed by rapid uplift and unroofing, which consequently may have lead to an uncompleted reset of the system. Although AFT data alone do not constrain the timing of exhumation for shallower surfaces, Bense et al. (2013) have used a different and more appropriate technique based on AHe dating obtaining non-reset AHe ages. Taken together, these results suggest that some positive topography may have already existed in this region prior to Neogene flat-slab subduction. Superimposed, a causal relationship has been proposed between southeastward propagation of exhumation in the Sierras Pampeanas and the shallowing of the subducted slab probably enhanced by the buoyancy of the Juan Fernández Ridge (JFR) lying on top of the Nazca plate (Coughlin et al., 1998; Yañez et al., 2001; Kay and Mpodozis, 2002).

In this paper we present apatite (U–Th)/He data from the Carboniferous-Triassic basin fill that is exposed in the structural hangingwall block of the northern SVF (Fig. 2) to complement the existing datasets in the Sierra de Valle Fértil. Existing AHe data in the northern, central and southern sector of the Sierra de Valle Fértil (Bense et al., 2013; Fosdick et al., 2015) are also used in this work. In addition, seismicity distribution patterns and neotectonic features are described to put constrains on how the SVF evolved in the last 5 Myr and how it is actually deforming.

2. Geological framework

The Sierras Pampeanas geological province is a wide morphotectonic region in the western-central part of Argentina, where continental deformation is observed more than 700 km east of the Chilean trench into the Andean foreland (González Bonorino, 1950; Jordan and Allmendinger, 1986; Kay and Mpodozis, 2002). In addition, there is a volcanic gap and a horizontal subduction of the slab between 27°S and 33°S with the most recent volcanism recorded in Pocho and Morro at 4 Ma and 1.9 Ma, respectively (Gordillo and Lencinas, 1981; Llambías and Brogioni, 1981) (Fig. 1). The Sierras Pampeanas region consists of a series of elongated N–S trending basement-cored uplifts that have structurally segmented the previously continuous Andean foreland basin (González Bonorino, 1950; Cardozo and Jordan, 2001). The whole morphostructural unit has been divided in western (WSP) and eastern (ESP) Sierras Pampeanas domains according to their lithology and metamorphic grade of the exposed rocks (González Bonorino,

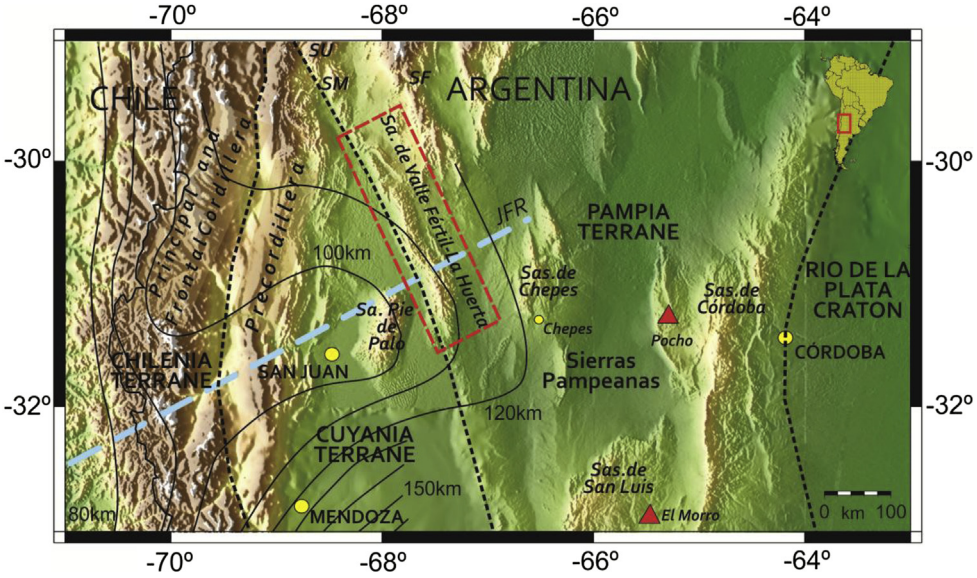

Fig. 1. Regional map of the Pampean flat-slab subduction zone showing terrane boundaries (dashed lines) and main morphostructural units from Ramos et al. (2002) and Rapela et al. (2007). Red triangles are expiring volcanic centers in the last 5 M.a. (Kay and Gordillo, 1994). Slab contours to the top of the Wadati-Benioff zone from Anderson et al. (2007) and the Juan Fernández Ridge (JFR) path according to Yañez et al. (2001) are also indicated. The red dashed-line rectangle represents approximate location of the study area shown in more detail in Fig. 5. (For interpretation of the references to colour in this figure legend, the reader is referred to the web version of this article.)

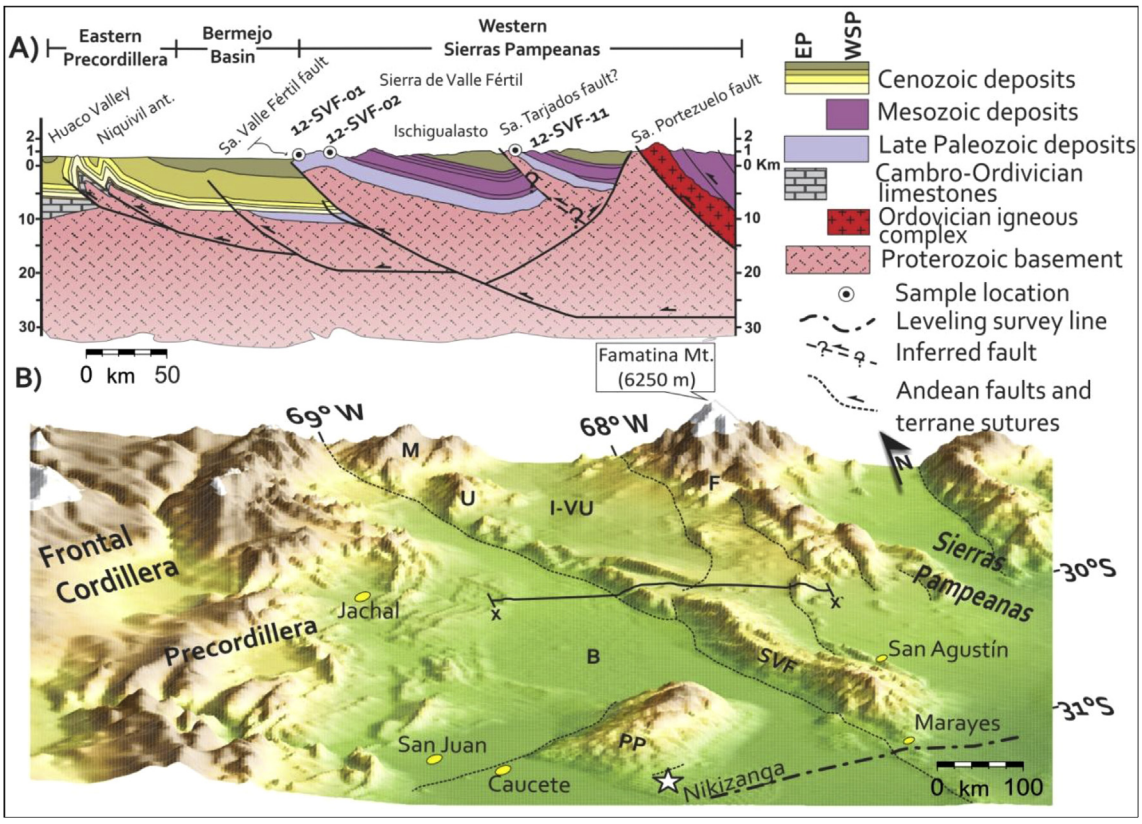

Fig. 2. A) Simplified schematic structural cross section along west-east line X–X′ in the northern Sierra de Valle Fértil based on Zapata and Allmendinger (1996); Rosello et al. (1996) and Lince et al. (2008). B). Digital elevation map of the Andean retroarc region around the Sierra de Valle Fértil (SVF) in west-central Argentina (Fig. 1) showing highest peak (Mount Famatina) in the western Sierras Pampeanas region, main Andean faults and terrane sutures after Vujovich et al. (2004). Solid black line indicates the location of the transect X–X′ along the northern Sierra de Valle Fértil shown in (A). Thick dashed line corresponds to region of leveling measurements in the epicentral area of the 1977 earthquake (star) by Kadinsky-Cade et al. (1985). Key to symbols: EP: Eastern Precordillera, WSP: Western Sierras Pampeanas, M: Sierra de Maz, U: Sierra de Umango, F: Sierra de Famatina, I-VU: Ischigualasto-Villa Unión basin, B: Bermejo basin, SVF: Sierra de Valle Fértil, PP: Sierra de Pie de Palo (see geological references in the text).

1950; Caminos, 1979). The ESP are composed of metamorphic and igneous rocks developed by accretion of different allochthonous and parautochthonous terranes during the late Proterozoic and the early Paleozoic that have been amalgamated into a larger cratonic block defined as the Pampia terrane (Ramos et al., 2002, 2010; Steenken et al., 2004; Miller and Söllner, 2005). This terrane underwent a complex history of deformation, metamorphism, and magmatism after its collision with the Rio de La Plata craton at the end of the Proterozoic. West of the Pampia terrane, the subsequent collision of the Precordilleran (Cuyania) terrane of Laurentian affinities (Astini, 2003) generated the Early Ordovician Famatinian arc in the south-western boundary of Gondwana (Rapela et al., 2007; Otamendi et al., 2009). Vestiges of this ancient magmatic arc are grouped as part of the WSP.

The SVF is one of the westernmost expressions of the WSP in Argentina (Fig. 2). The north and south edges of the crystalline basement-cored of the SVF are overlain by thick sequences of Triassic sedimentary rocks corresponding to the ~2500-m-thick Ischigualasto and ~1500-m-thick Marayes basins, respectively (Milana and Alcober, 1994; Malizia et al., 1995; Spalletti, 1999). The western flank of the range is bounded by the east-dipping Valle Fértil reverse fault system that places in contact basement rocks over the Bermejo valley strata (Snyder et al., 1990; Zapata and Allmendinger, 1996). The same region has been proposed to be the place of a suture between the Cuyania and Pampia terranes (Snyder et al., 1990; Ramos, 1994; Castro de Machuca et al., 2008).

Andean deformation associated with the Sierras Pampeanas region propagated from west to east during the past 10 Myr (Malizia et al., 1995; Ramos et al., 2002) and agrees well with the migration of magmatism away from the trench as the slab flattened (Kay and Abbruzzi, 1996; Kay and Mpodozis, 2002). It is worth to note, that deformation and magmatism not only had migrated laterally from west to east but also from north to south in association with the shallowing of the subducted slab (Coughlin et al., 1998) and the path of the JFR beneath South America in the last 15 Myr (Yañez et al., 2001; Ramos et al., 2002). Because the SVF extends more than 180 km along a NW–SE trending orientation within the WSP, we suggest its deformational and exhumational history could help to test for any lateral migration of deformation along-strike.

The Sierras Pampeanas have been proposed as uplifted by deep high-angle reverse faults, which correspond to the inversion of former Triassic and Cretaceous extensional faults (Jordan and Allmendinger, 1986; Introcaso et al., 1992; Ramos et al., 2002). The extensional faults and associated rift basins are related with the opening of the South Atlantic Ocean (Uliana et al., 1989; Rossello and Mozetic, 1999). According to Ramos et al. (2002), master extensional faults were generated by reactivation of the sutures between previously accreted terranes, resulting in formation of continental rift basins, usually with half-graben geometries and most of the deformation taking place in hangingwall blocks. Recent seismological results have imaged some decóllement mid-crustal levels in the SVF region (Gallardo, 2011; Ammirati et al., 2015). Thus, the Sierra de Valle Fértil fault in the WSP and the related

Ischigualasto-Villa Unión and Marayes eastern basins could be good candidates for accommodating actual deformation (Fig. 1) (Criado Roque et al., 1981; Aceñolaza and Toselli, 1988; Ramos et al., 2002).

3. Analytical methodology

3.1. Apatite (U–Th-Sm)/He thermochronology

(U–Th-Sm)/He thermochronology is based on the accumulation of ^{4}He produced during the radioactive decay of ^{238}U, ^{235}U, and ^{232}Th in apatite crystals (Zeitler et al., 1987; Wolf et al., 1996; Farley, 2002). ^{4}He gas is highly mobile at temperatures above 80 °C and, due to its mobility, is lost through diffusion out of the crystal lattice. However, below 55°C, apatite begins to retain daughter ^{4}He and consequently it is accumulated in the crystal lattice during rock exhumation to the surface. This range of temperature, where ^{4}He is partially retained, is known as the Partial Retention Zone (PRZ) (Wolf et al., 1996; Farley, 2002; Reiners et al., 2004). Conventionally, He diffusion in apatite is assumed to be sensitive to temperatures from ~70 to 30°C (Wolf et al., 1998). However, recent studies demonstrated that He retentivity increases with the accumulation of He and associated radiation damage in the apatite crystal, such that an apatite's effective closure temperature evolves through time (Farley, 2000). Forward models predict that for some thermal histories and apatite suites, the radiation-damage effect will be manifested as a span of (U–Th)/He dates positively correlated with both He concentration [He] and effective U concentration [eU]. The latter parameter [eU] weights the decay of U and Th for their He productivity, and is computed as ([U] + 0.235 × [Th]). Our data shows a positive correlation between date and [eU] (Fig. 3), which develops because an older apatite with higher [eU] and more radiation damage has a higher closure temperature than a lower [eU] (younger) apatite with less radiation damage, despite experiencing the same thermal history.

Due to the thermal sensitivity (55°C–80°C) of the apatite (U–Th-Sm)/He system, subsequent heating due to burial or elevated geothermal gradient can cause He loss and resetting of the sample. This property is particularly useful for sedimentary samples in this study, because the thermochronometric results can be used to evaluate the post-depositional heating of basin infill and subsequent cooling and inferred exhumation during uplift. If a sedimentary sample yields a completely reset AHe date, it means that post-depositional burial heating was sufficient to degas the sample well above the closure temperature, which causes complete resetting of the original cooling signal due to the diffusive loss of He. On the other hand, a sedimentary sample that has undergone only moderate heating within the temperatures of the PRZ, is characterized by a range of apparent dates that are younger than the depositional age. Finally, an unreset sample represents a sedimentary sample that has remained below the PRZ temperature window and, therefore, will preserve information about the cooling of the source rock from which the sediment was eroded.

In all the cases described above, we obtained the thermal history using HeFTy code by Ketcham (2005), which generates both forward and inverse models for low-temperature thermochronometric systems. The forward model allows the user to calculate the expected data distribution for any given thermal history, whereas the inverse model finds the thermal history that best matches the input data. Only samples with acceptable results of helium and effective uranium concentration, as well as, a factor correction (Ft) $\geq$ 4 were modeled (Table 1). Initially, forward modeling of single grain age was performed. Constraints involved uncorrected age, alpha calculation, radius of the mineral, among other factors. Once thermal history is generated for each grain, they are run synchronously with the purpose to do an inversion for the time-temperature history, thus generating a set of thermal histories that are considered consistent with observations for each sample. This is evaluated using the goodness-of-fit (GOF) parameter between predicted and observed data distributions (Ketcham, 2005) (Fig. 4). Because no thermal history ever uniquely defines a set of AHe data, the better fitting thermal histories must always be considered in the context of local geological constraints. For that reason user can set initials and final conditions, like constraints on the time and temperature of deposition or crystallization and ending temperature-time (e.g. samples extracted for boreholes have a different temperature constrain from samples at the surface). User can include geologic evidences at the field and other thermochronological data. Furthermore, user can also decide how many paths should be tried before start the modeling. The more paths tried, the more accurate the T–t history obtained will be. Finally, the program allows to display the thermal history as paths, path envelopes (this work) or constraining points (Fig. 4).

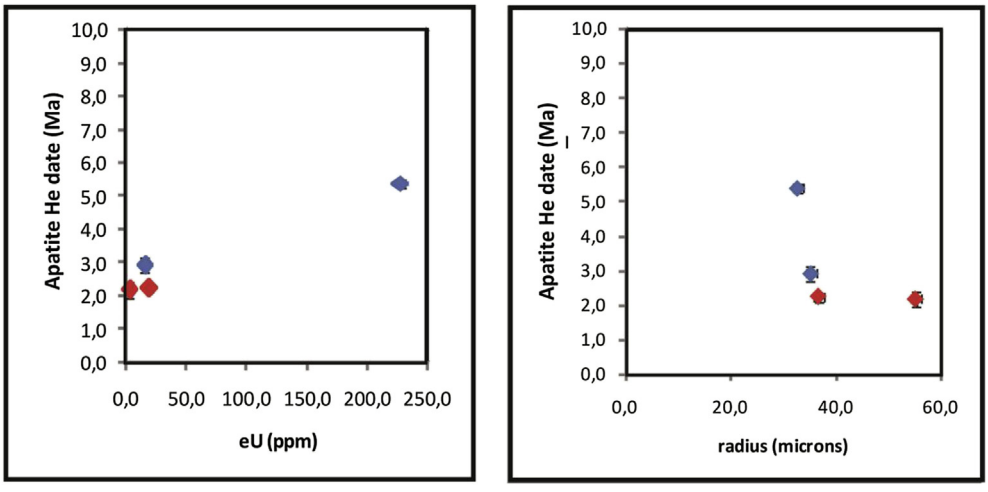

Fig. 3. Apatite (U–Th)/He results for Samples 12-SVF-02 (blue) and 12-SVF-11 (red) from this study at the northern Sierra de Valle Fértil (see Fig. 2A for location). (Left panel) Relationships between obtained dates and effective uranium concentration (eU). (Right panel) Same ages versus effective grain radius. Positive correlation between AHe date and effective uranium concentration (eU) probably indicating that burial heating was sufficient to partially reset apatites with low eU values. (For interpretation of the references to colour in this figure legend, the reader is referred to the web version of this article.)

Table 1
Apatite thermochronology data.

Sample	Latitude (°S)	Longitude (°W)	Elevation (m)	Grain	Lithologic unit	Effective radius (μm)	U (ppm)	Th (ppm)	Sm (ppm)	eU (ppm)	Th/U	He (nmols/g)	Ft	Single grain age (Ma ± 2σ)	Weighted mean age (Ma ± 2σ)
12-SVF-02	−30.14255	−68.03188	898	Ap1	Carboniferous Paganzo Group Sandstone	35.3	13.79	7.70	52.2	15.6	0.558	0.15	0.61	2.9 ± 0.2	4.7 ± 0.5
				Ap4		32.8	169.42	246.96	180.0	227.5	1.458	3.78	0.59	5.4 ± 0.1	
12-SVF-11	−30.16310	−67.84159	1374	Ap2	Triassic Ischigualasto Fm. Sandstone	55.3	1.32	6.30	4.3	2.8	4.778	0.02	0.74	2.2 ± 0.2	2.2 ± 0.4
				Ap3		36.8	10.73	35.55	66.3	19.1	3.314	0.14	0.63	2.2 ± 0.1	

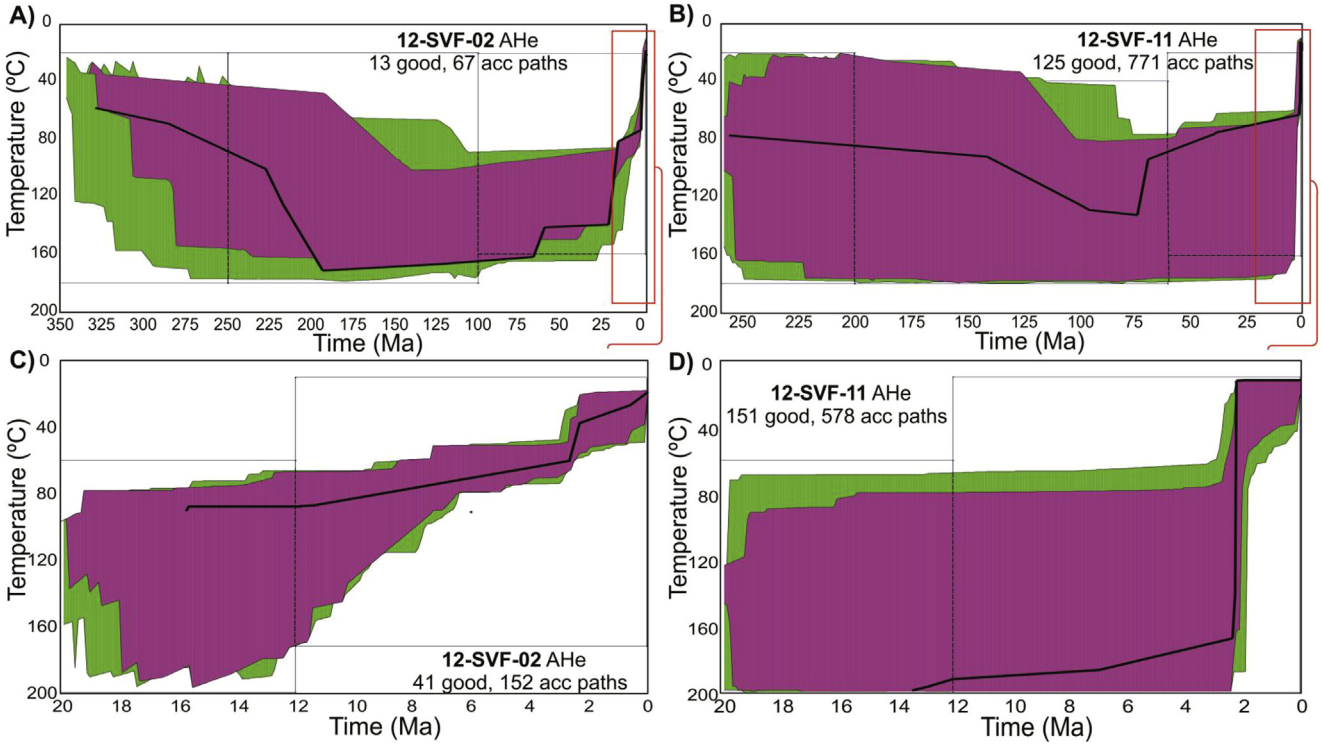

Fig. 4. Four inverse modeling results for two key samples (A) 12-SVF-02 and (B) 12-SVF-11 from the Sierra de Valle Fértil hanging wall (see location of the samples in Figs. 2 and 5). The results are displayed as Temperature versus time (T–t) envelope paths for good (magenta), acceptable (green) and best fit (solid black line) histories. Models (A) and (B) exhibit attempted 100,000 and 50,000 T–t paths, whereas (C) and (D) represent 50,000 and 10,000 T–t paths, respectively. Dark grey boxes indicate the imposed T–t constraints, which were chosen following geological evidence criteria. For (A) and (B), initial modeled boxes consider depositional ages and surface Temperatures; for (C) and (D), initial modeled boxes consider starting Temperatures ≥ 60 °C due the resetting of the system, and final boxes with present day surface Temperatures. See text for more details. (For interpretation of the references to colour in this figure legend, the reader is referred to the web version of this article.)

3.2. Sample suite

For this study, samples were collected in a west-east transect of the northern part of SVF in order to assess changes in timing and rate of cooling across the SVF hangingwall block. Although more than ten samples were collected in the field, only few of them have met the quality requirement criteria, i.e. containing large euhedral and inclusion-free apatite grains suitable for analysis. Obtained grain radius range from 32.8 μm to 55.3 μm (Table 1 and Fig. 3). Samples consist mainly of sedimentary rocks from the Paleo-Mesozoic Ischigualasto-Villa Unión basin in the north of Sierra de Valle Fértil (Figs. 2 and 5). Sample 12-SVF-02 was obtained in outcrops near the sierra de Valle Fértil thrust fault corresponding to fluvial-deltaic sandstone beds from the Carboniferous Guandacol Formation, while sample 12-SVF-11 was obtained from outcrops of fluvial sandstone strata from the Triassic Ischigualasto Formation, exposed near Ischigualasto basin. We also compiled a synthesis of existing low-temperature thermochronology data from nearby sampled outcrops by Bense et al. (2013) and Fosdick et al. (2015).

3.3. Sample preparation

Sample preparation and gas extraction were carried out in the Arizona Radiogenic Helium Dating Laboratory (ARHDL) at the University of Arizona (U.S.A.). Apatite grains were isolated using standard magnetic and density separation techniques and were carefully hand-selected under cross-polarized light to avoid U- and Th-rich mineral and fluid inclusions (e.g., zircon, monazite) that may produce errors in the apatite ages due to excess of helium. Images of selected grains were captured by a closed-circuit digital video camera mounted on the microscope and measured using analysis techniques for the purposes of an alpha ejection correction calculation (Farley and Wolf, 1996). Selected crystals (n = 2–3 grains per sample) were degassed under vacuum using laser heating and analyzed for He using a quadrupole mass spectrometer. Following He measurements, the crystals were analyzed for

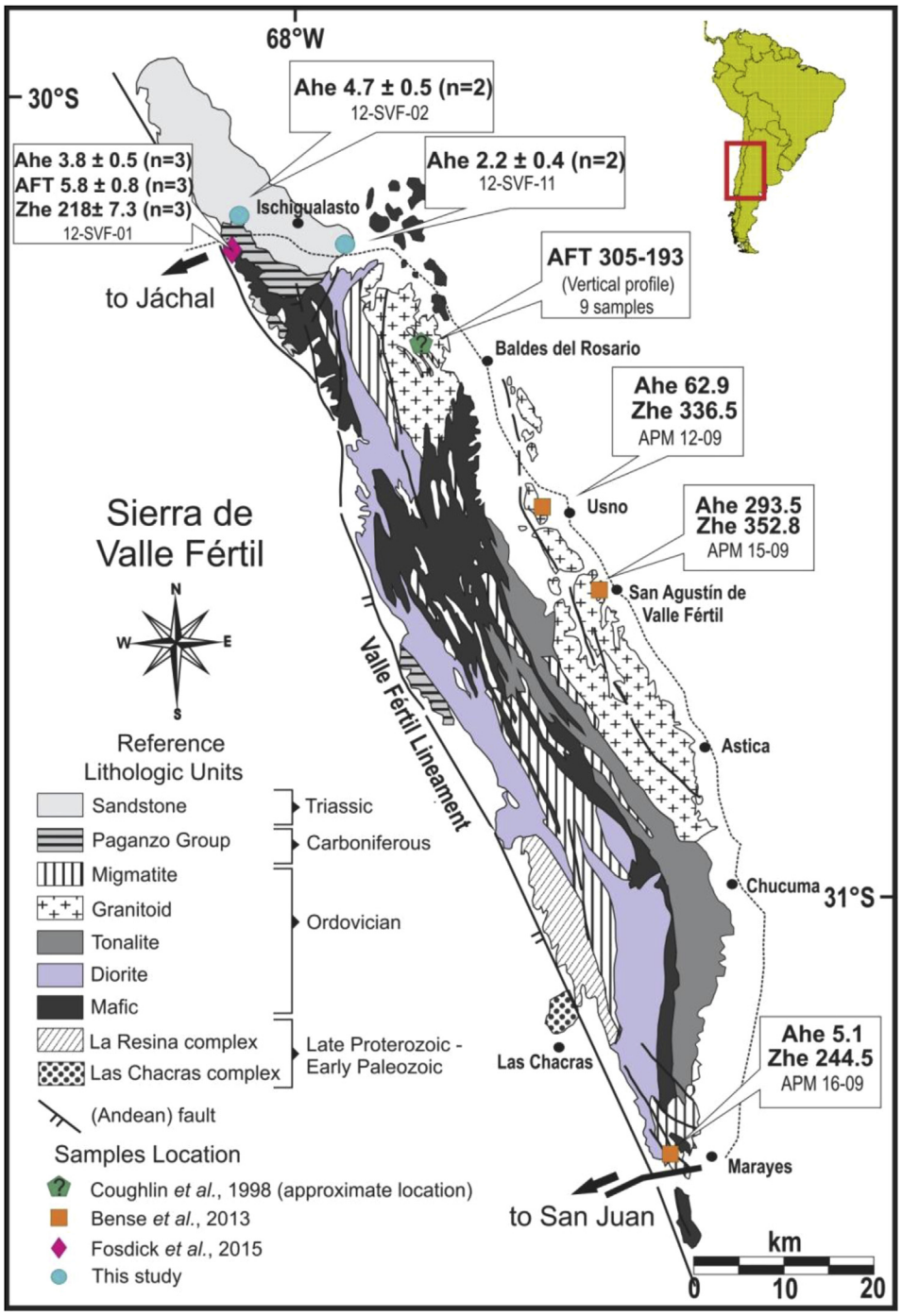

Fig. 5. Simplified geological map of the Sierra de Valle Fértil (modified from Otamendi et al., 2009) showing sample locations and AFT, ZHe and AHe ages discussed in the main text. Errors quoted throughout as two standard deviations (2σ) of weighted mean AHe ages as well as number of analyzed grains (n) are also indicated for samples in the north of SVF.

determining U and Th abundances by using inductively coupled plasma-mass spectroscopy (ICP-MS) through isotope dilution following Reiners and Nicolescu (2007)ś methods.

3.4. Thermochronologic data modeling

Inverse modeling of AHe data from the SVF helps us to better understand the Temperature-time (T–t) history of the region. As stated above, AHe ages were modeled using the HeFTy program (Ketcham, 2005), which can calculate solutions for up to seven different thermochronometers simultaneously. The kinetic model used for apatite (U–Th-Sm)/He is the radiation damage accumulation and annealing model (RDAMM) after Flowers et al. (2009). Modeled Temperature-time paths for two samples taken from the north of the SVF are shown in Fig. 4. Input data for the modeling were the apatite (U–Th)/He dates, U and Th concentrations, and effective grain size. We assumed T–t conditions for the modeling on a base of the geological history from field observations and previous ZFT, ZHe, AFT and AHe data. We performed four different models for two key samples from the SVF. The main difference between the models is the used time lag constrain. Thus, for sample 12-SVF-02 (Table 1 and Fig. 2) we have used in the modeling a time

period of 350 Ma to present (Fig. 4A), and another younger time period corresponding to the last 20 Myr (Fig. 4C). The same tests were performed for sample 12-SVF-11 (Fig. 4B and C).

Two grains from sample 12-SVF-02 from Carboniferous Guandacol Fm. Sandstone were modeled simultaneously at different selected time intervals: an older T–t window (180–20 °C for 350–250 Ma), which includes the sediment deposition; an intermediate T–t window (180–60 °C for 250–100 Ma); and a shorter T–t window (160–20 °C for 100–0 Ma). Modeling of two grains for sample 12-SVF-11 from Triassic Ischigualasto Fm. sandstone followed a similar analysis. In this case we tested three different T–t intervals: an older T–t window of 180–20 °C for 260–200 Ma, which covers its depositional age; an intermediate T–t window of 180–40 °C for 200–60 Ma; and a younger T–t window of 160–20 °C for 60–0 Ma. A final temperature at the surface of 20 °C was considered for both sample analyses.

4. Results

Our results for two samples from the northern region of the Sierra de Valle Fértil using apatite (U–Th-Sm)/He dates (AHe dates) help to complete a low-temperature thermochronologic dataset between 30°S and 31.5°S for this range (Figs. 1–5). Errors are quoted throughout as two standard deviations (2σ) as uncertainties of weighted mean ages. The main difference between AHe ages obtained in this study and those from Bense et al. (2013)ś dataset is that we calculate weighted mean dates from the single-grain dates, whereas ages from Bense et al. (2013) are a simple average. Thus, our 'mean dates' are actually weighted mean dates, so grains with smaller uncertainties (i.e. better measurements) will have higher control over calculated mean. Measured single-grain AHe dates from Samples 12-SVF-02 and 12-SVF-11 (n = 2 grains per sample) showed relatively young cooling ages (Table 1), indicating a complete post-depositional resetting prior to Pliocene-Pleistocene exhumation. Westernmost sample 12-SVF-02 yields a weighted mean AHe age of 4.7 ± 0.5 Ma. At the eastern border of the SVF close to Ischigualasto (see location in Figs. 2 and 5), sample 12-SVF-11 yields a weighted mean AHe age of 2.2 ± 0.4 Ma.

Modeled T–t paths for the two samples in this study at northern SVF clearly indicate both samples share a recent thermal history (Fig. 4A and B). For this reason, a second modeled T–t history was performed within the last 20 Myr to gain more insight on time of final cooling (Fig. 4C and D). Comparatively, modeling history from sample 12-SVF-02 shows more heating in early stages during late Paleozoic–Mesozoic than that one for sample 12-SVF-11; this agrees well with their different burial vertical stratigraphic position caused by deposition of Triassic sediments from the Ischigualasto basin. Thus, the westernmost sample 12-SVF-02 reached deeper depth levels than the easternmost sample 12-SVF-11. At Cenozoic, both samples followed similar periods of monotonic cooling in late Cretaceous – early Cenozoic, although at higher temperatures for sample 12-SVF-11. We note, however, that best fit paths exhibit an abrupt cooling period within the last 2 Myr.

Since AHe dates are substantially younger than depositional ages, we state all AHe dates to have been completely reset, yielding closely clustered dates as seen in Fig. 3 and Table 1.

5. Previous thermochronology observations in the sierra de Valle Fértil

Previous low-temperature thermochronology studies in the SVF document a complex thermal history with multiple phases of cooling and possible reheating episodes. Apatite (U–Th-Sm)/He, zircon (U–Th-Sm)/He (Bense et al., 2013) and apatite fission track (AFT) (Coughlin et al., 1998) results from the central part of the Ordovician crystalline cored basement of the SVF suggest that this region of the Sierras Pampeanas underwent cooling through these closure systems ca. 293-63 Ma, 353-245 Ma and 305-193 Ma, respectively. These pre-Cenozoic thermochronology determinations provide a first-order constraint on the magnitude of cooling and exhumation related to the thermal condition of the samples prior to Andean deformation. These pre-Cenozoic AHe, ZHe and AFT ages may be showing an inherited age that has not been resetting or annealing and hence those rocks remained near surface prior to Andean exhumation. Furthermore, a sample from Carboniferous strata from the northern foothills of the SVF hanging wall showed a Permian ZHe date, suggesting that the basin infill has not been sufficiently buried to reset ZHe ages as occurred for AHe, ZHe and AFT in the central part of the SVF. However latest Miocene–Pliocene cooling and exhumation were showed for this Carboniferous sample through both the AFT and AHe partial retention zones occurring between 5.8 ± 0.8 Ma and 3.8 ± 0.5 Ma, respectively (Fosdick et al., 2015).

6. Discussion

The northern termination of the SVF and other minor ranges extending northward have been propose to disrupt the already formed Bermejo foreland basin during the Neogene giving the current configuration for Bermejo and Ischigualasto-Villa Unión adjacent basins. Malizia et al. (1995), Jordan et al. (2001), among others have roughly constrained the ages of exhumation of these western Pampean Ranges by conducting chronostratigraphic, paleoenvironmental, and tectonics analyses on Neogene sedimentary deposits. The Pliocene AHe ages in this work allow us to better constrain the exhumation history of the SVF Pampean range, which is in good agreement with the hypothesis of the uplift of the Sierras Pampeanas region during slab flattening of the Nazca plate beneath South America. In this view, enhanced coupling between the plates may have reactivated Pampean reverse faults, causing increasing topography that was subject to erosion and continue active to the present as shown by high level of crustal seismic activity (Alvarado et al., 2005) and neotectonic features (Bastias, 1985; Costa et al., 2000; Siame et al., 2005; Perucca and Vargas, 2014) (Figs. 6 and 7).

In the last decades a wide variety of regional studies carried out in the Sierras Pampeanas region of west-central Argentina allowed to constrain a roughly eastward propagation of increased exhumation within the south-central Andes backarc. Stratigraphic data (Strecker, 1987) and AFT studies (Coughlin et al., 1998) have focused around 28°S and estimate the main uplift of the Sierra de Aconquija between 7.6–6.0 and 4.0–3.4 Ma (Ramos et al., 2002). Southward (29°S), magnetostratigraphic (Tripaldi et al., 2011) and isotopic records (Losada-Calderón et al., 1994; Tosselli, 1996) suggest the beginning of the uplift at Sierra de Famatina (Fig. 2) between 4.5 and 4.2 Ma (Ramos et al., 2002). In the north area of the Sierra de Valle Fértil, foreland basin studies in the adjacent Bermejo and Ischigualasto-Villa Unión basins recorded an interruption in the sedimentation of the distal wedge of Bermejo basin at about 4.3 Ma likely associated to the uplift of the SVF and other minor ranges extending northward (Johnson et al., 1986; Malizia et al., 1995). Recent studies by Siame et al. (2015) more to the south in the Western Sierras Pampeanas (31°S), used in-situ cosmogenic radionuclide and geomorphological data from the Sierra de Pie de Palo (see Figs. 1, 2 and 6) to determine the initiation of uplift between 4 and 6 Ma; the same studies suggest that it continues to present day with a shortening rate of about 4 mm/yr and an uplift rate of 1 mm/yr (Ramos and Vujovich, 2000). All these previous results are in agreement with the broken foreland of Argentina hypothesis proposed for the last 15 Myr (Zapata and Allmendinger, 1996; Ramos and Folguera, 2009), the migration of magmatism in

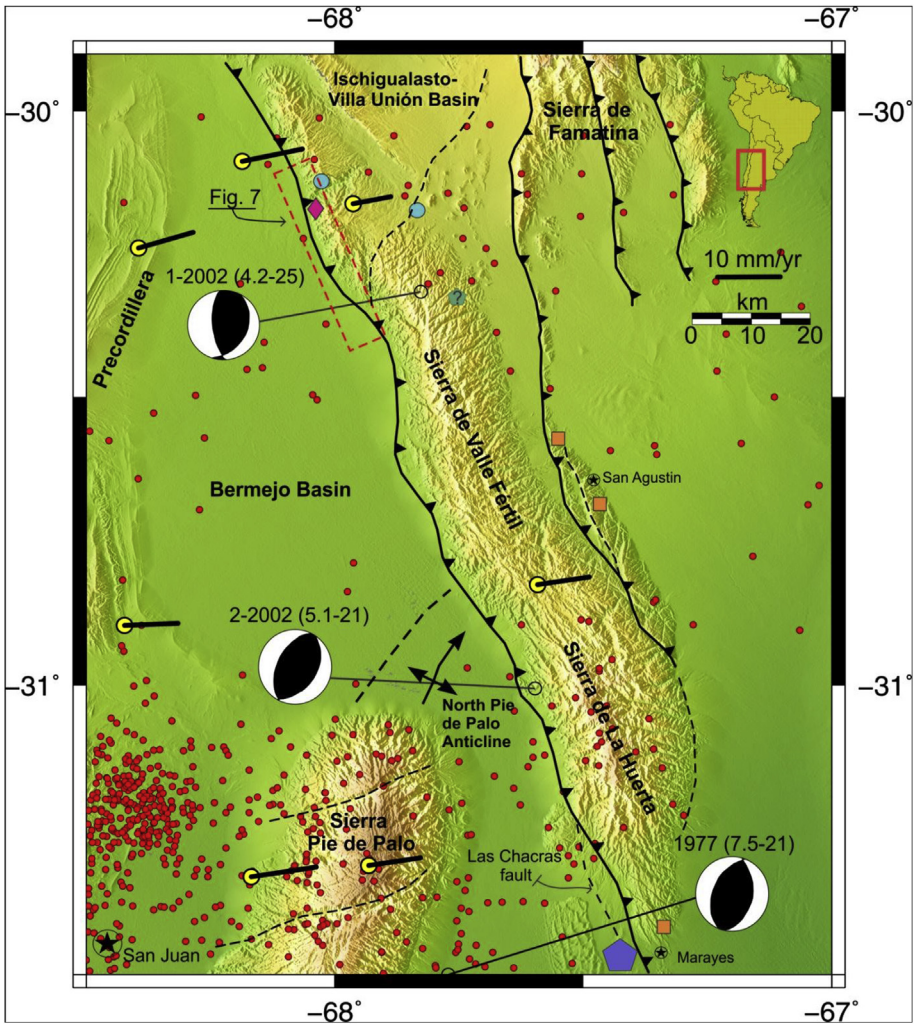

Fig. 6. Local crustal seismicity of magnitude M ≥ 3 from INPRES (2015) during three years (red dots). Also shown, are focal mechanisms by Alvarado et al. (2005) obtained using broadband seismic waveform modeling; earthquakes are represented by year of occurrence, and magnitude Mw-focal depth in km in parenthesis. The 1977 event corresponds to the large (Mw 7.5) Caucete crustal earthquake (Langer and Hartzell, 1996). The pentagon near Marayes shows location for accommodation of 0.4 m slip vertical motion along the SVF thrust fault after the 1977 earthquake according to leveling measurements (Kadinsky-Cade et al., 1985). GPS velocity vectors are from Brooks et al. (2003). Abbreviations, other symbols and references as in Fig. 3. Location of Fig. 7 (red dashed-line rectangle) showing neotectonic observations is also indicated. (For interpretation of the references to colour in this figure legend, the reader is referred to the web version of this article.)

the Andean backarc (Kay and Mpodozis, 2002) and subduction in a more west-east orientation of the JFR in the last 10 Ma (Yañez et al., 2001).

The Precordillera -Western Sierras Pampeanas interaction is well known by being an active seismogenic region in western Argentina. This zone has produced the most devastating earthquakes in Argentina history (Langer and Hartzell, 1996; Alvarado and Beck, 2006). Larger magnitude-sized earthquakes have produced relatively large fault rupture segments in the basement; in addition small to moderate seismicity continuously produces earthquake deformation consistent with an east-west compression stress regime in the Andean backarc (Siame et al., 2005; Monsalvo et al., 2014; Allmendinger and Judge, 2014). Although very sparse geological studies have focused in the Sierra de Valle Fértil, we provide evidence that north and south low elevation edges of the SVF shared not only young AHe ages but also higher levels of seismicity (Fig. 6) and Quaternary alluvial fans being affected by neotectonic features (Fig. 7); hence the importance of conducting thermochronology studies in the topographically subdued but active range terminations, both in the crystalline and sedimentary rocks.

6.1. Low-temperature thermochronology and tectonic interpretation

Given a geothermal gradient of 20–30°C/km, the closure temperature of ~80°C for (U–Th-Sm)/He system will be located around 2–3 km below surface. Due to the reset ages obtained on AHe data for this and previous studies, we propose that at least 2–3 km of erosion of Neogene sediments north and south of the SVF is clearly associated with Cenozoic Andean exhumation, assuming monotonic cooling. In correspondence with our determinations, Jordan et al. (2001), making used of compiled data from well sections and industry seismic lines, inferred the northern termination of SVF being buried bellow >3 km of Neogene sediments during the formation of the Bermejo foreland basin between 20 and 2.8 Ma, i.e. before to be divided by the north SVF and other minor northern Pampean range uplifts (e.g., Johnson et al., 1986; Reynolds, 1987; Malizia et al., 1995).

For samples that yield older AHe ages at the central region of the SVF (Bense et al., 2013), we hypothesize that they could represent (a) areas of only partial resetting during protracted residence in AHe PRZ prior to the onset of cooling, and/or (b) these regions were

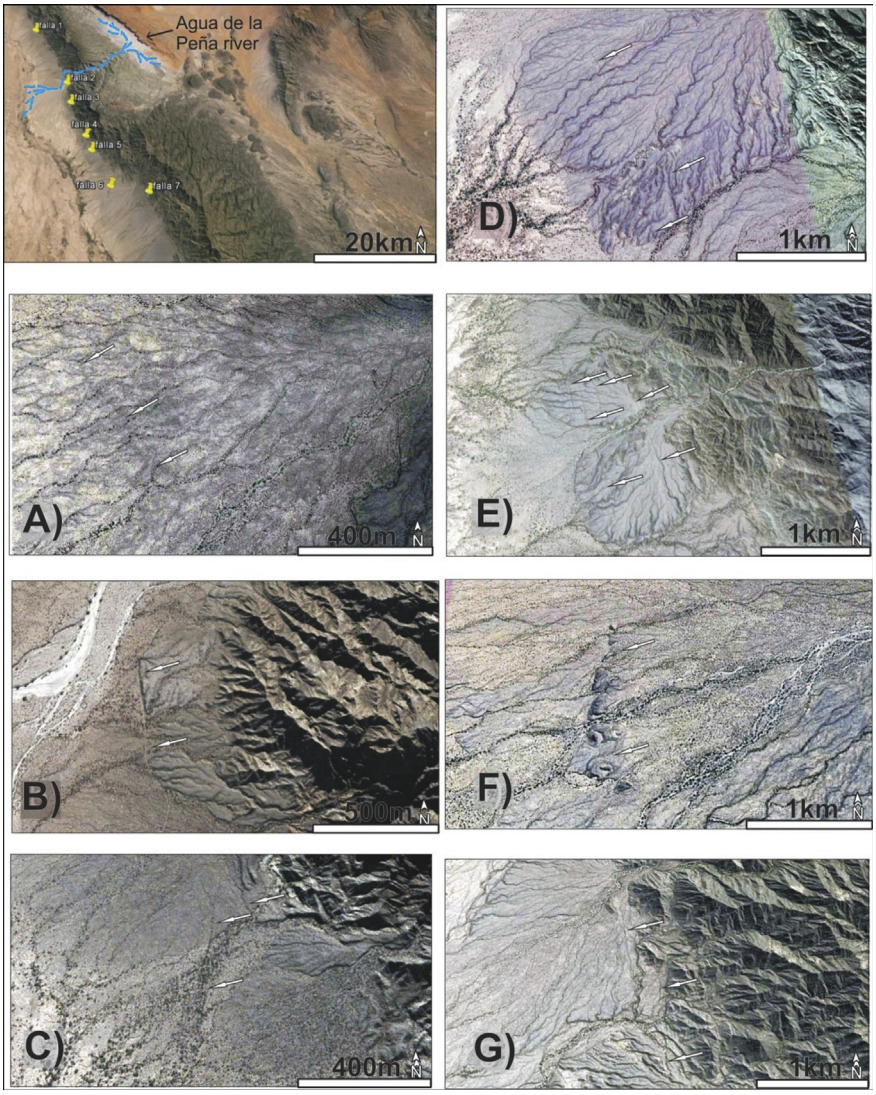

Fig. 7. Top right figure shows *Google Earth* image of the northern end of the Sierra de Valle Fértil Fault System in the western piedmont of the SVF mountain range as indicated in Fig. 6. A zoom for the area around each pin from northwest to southeast is shown in figures (A) to (G) using white arrows to denote recent scarps affecting alluvial deposits: A) *Preferential slope in ~330°-trending scarps affecting Pleistocene-Holocene alluvial fans;* B) N–S trending on west-facing scarp located to the south of the Agua de La Peña river. We note that temporary streams coming from the Sierra de Valle Fértil are definitely more incised in the hanging block; C) N10°-trending fault scarp affecting Holocene alluvial deposits; D) Parallel traces of 170° tending affecting several Quaternary alluvial levels. Unpaired terraces are associated to the hanging block; E) Discontinuous trace of a 330° trending preferential-slope scarp; F) Fault scarp of N–S trending, showing its free face to the W with the maximum height of the fault system; G) Approximate N–S trending scarp affecting at least two Quaternary terraces and alluvial levels.

remnant positive relief prior to Cenozoic Andean tectonics.

(a) Structurally, the SVF and northern minor Pampean ranges shared the feature of the doubly plunging asymmetrical folded terminations. In addition, besides sharing an analogue basement-involved deformation, the SVF in the Sierras Pampeanas also shares a similar pattern of deformation observed for some ranges in the Rocky Mountains of North America. Crowley et al. (2002) carried out apatite (U–Th)/He thermochronology studies in the Bighorn Mountain range, and found old pre-Laramide AHe ages in the center of the range that decrease toward the edges. In their investigations a structural model for the range involves its basement folded along-strike and parts of the range bearing the pre-Laramide AHe remained near surface and below apatite (U–Th)/He closure temperature (~70°C) prior to Laramide exhumation; whereas the edges remained above apatite PRZ (~85°C), resetting the AHe system and showing Laramide ages. It is worth to note that this antiform-like style of deformation is shared among the Western Sierras Pampeanas of San Juan and La Rioja province. As the antiform grows and is uplifted, the exhumation begins at the center first and then progressively exhumes toward its edges. According to this pattern of exhumation the range will show a decreasing age progressively from the oldest ages in the center to the youngest ages toward the edges. The hypothesis of a long permanence in the PRZ is reliable but it is hard to prove it with scarce AHe data.

(b) The other hypothesis that the Sierras Pampeanas and other regions of South America have developed a positive relief during most of the Phanerozoic time has attracted attention in the last decades. Evidence for Gondwana paleosurfaces has been proposed on a base of multiple studies as development of deep weathering soil profiles and formation of

etchplains, recognition of uncovered relict landscapes and planation surfaces (Rabassa et al., 2010), low-temperature thermochronology (Dávila and Carter, 2013; Löbens et al., 2013; Bense et al., 2013), among others. The creation of this paleorelief has been estimated between the middle Jurassic and the Paleogene. Due to Neogene sediments are not found in the central body of the SVF range, it is possible that this central peak area may be acting as a sediment source for the adjacent basins by the time of Bermejo foreland basin was under formation. The fact that Pliocene AHe ages are found in the northern and southern terminations of the SVF (Bense et al., 2013 and this study), as well as in the southern edge of the Sierra de Pie de Palo (Löbens et al., 2013) provides evidence for the influence of Andean tectonics and exhumation at the edges of these western Pampean Ranges.

6.2. Seismicity and new hints on the west piedmont of the Sierra de Valle Fértil deformation

The Western Sierras Pampeanas represent one of the most seismically active regions in Argentina, generating damaging shallow crustal earthquakes that have caused deaths and serious economic consequences in Argentinean history (INPRES, 2015). The latest large earthquake has occurred in the Sierra de Pie de Palo eastern flank near Caucete, San Juan on 23 November 1977, killing 63 people (INPRES, 2015, Figs. 2 and 6). Teleseismic waveform modeling from this (Mw 7.5) earthquake showed its seismic source was composed of two shocks rupturing multiple faults and basement blocks, and separated by a horizontal distance of about ~65 km and 20.8 s (Kadinsky-Cade, 1985; Langer and Hartzell, 1996). In addition, those studies illustrate how their aftershocks and associated coseismic deformation propagated across a broad area involving the Sierra de La Huerta, which is the southern prolongation of the SVF (Figs. 1 and 6). Estimation of displacements after the 1977 earthquake using precise leveling data indicated not only the Sierra de Pie de Palo but also the Sierra de La Huerta itself located more to the east is responsible for about 0.5 m of slip accommodation on a high-angle (~65°), shallow (~6 km) east dipping fault (Kadinsky-Cade et al., 1985; Langer and Bollinger, 1988).

Modern seismicity studied by local experiments using local temporary and permanent seismic stations in the region shows a higher concentration of relocated epicenters in the north and south SVF crust (Venerdini, 2014). Seismic moment tensor inversion solutions for two moderate crustal earthquakes in 2002 shown in Fig. 6 using complete broadband three-component regional waveform modeling recorded by the CHARGE experiment (Beck et al., 2001) indicate magnitudes and focal depths of Mw = 4.2; h = 25 km for Event 1-2002 in the north SVF, and Mw = 5.1; h = 21 km for Event 2-2002 in the SVF at 31°S, respectively (Alvarado et al., 2005). Interestingly, their focal mechanism solutions and focal depths agree with seismically active mid-crustal levels within a ~50-km-thick crust constrained by receiver functions, surface wave dispersion (Alvarado et al., 2009; Gans et al., 2011) and oil seismic reflection analyses (Zapata and Allmendinger, 1996). Total crustal thickness varies from about 50 km in the WSP to 35 km to the east of SVF (Ammirati et al., 2015) and several basement structures near the SVF fault like the buried north Pie de Palo anticline (Zapata, 1998) (Fig. 6), which seems to be seismically active. In addition, two discontinuities in seismic velocities have been observed at ~12 km and ~28 km depths beneath the Sierra de Valle Fértil (Gallardo, 2011). Bouguer anomaly studies in the Bermejo basin and SVF by Lince et al. (2008) are consistent with previous structural models for the SVF proposed by Rosello et al. (1996) illustrating a flower structure with a detachment level located around 22-km depth. In their interpretation, this structure likely inherited from Triassic rifting in the region could have been reactivated later by the Andean compression (Ramos, 1994; Ramos and Folguera, 2009).

Comparison of GPS velocity vectors in the region clearly shows an important decay from west to east across the north SVF fault (Brooks et al., 2003) (Fig 6). Horizontal shortening of about 86 km in the past 13 m y. as well as thickening seem to be occurring beneath the thin-skinned Precordillera at ~30°S. Average strain rate from Miocene to Holocene fault-slip data used in balanced cross-sections is indistinguishable from GPS strain rate (Allmendinger and Judge, 2014). Observation from those studies and Fosdick et al. (2015) using independent data indicate a progressive eastward migration of the thrust front through time as earlier proposed by Jordan et al. (1993) and Brooks et al. (2003) (Fig. 6).

Quaternary shortening in northern Sierra de Valle Fértil produced reverse-displacement reactivation of Mesozoic normal faults and structural inversion of Ischigualasto basin strata (Zapata and Allmendinger, 1996). Carboniferous and Triassic rocks are exposed in the hangingwall of the sierra de Valle Fértil Fault interpreted as reverse reactivated Triassic normal faults (Milana and Alcober, 1994; Zapata and Allmendinger, 1996). The ~N30°W trending sierra de Valle Fértil Fault system seem to have controlled the continuous basement uplift of the Sierra de Valle Fértil-La Huerta and other ranges along 600 km in the Western Sierras Pampeanas in the modern Pampean flat slab segment of the Andes (Snyder et al., 1990).

Neotectonic structures and Quaternary active faulting are shown along the northern and southern western-bounding fault of the Sierra de Valle Fértil-La Huerta (Perucca and Vargas, 2014). Specifically, at the northwestern SVF piedmont a variety of discontinuous parallel or suparallel to the mountain front fault traces, are observed disrupting Quaternary alluvial fans with scarps facing west (Fig. 7). The fault scarp heights vary along the fault system between few centimeters to ~10 m, showing the highest elevations in its central section.

The best exposed geomorphic evidence and most recurrent expressions of Quaternary tectonic activity from northern SVF are anomalies in drainage patterns, scarps and alluvial terraces, which are entirely located in the hanging block (Fig. 7). The SVF fault system traces exhibit a trend perpendicular to the streams coming from the mountain, so incision in the hanging block has occurred in response to recent uplift (Fig. 7b). Besides, terraces increase progressively in height above present channels (Fig. 7 g). Fig. 7e shows at least five subparallel scarps, characteristic of thrust where slip is distributed on multiple imbricate faults (McCalpin, 2009). In the southern prolongation of the SVF, the Holocene Las Chacras active fault strongly affects the western piedmont of this range (Rothis et al., 2012) (Fig. 6). Its fault traces can be followed for a distance of about 40 km. Taken together, all the observations described above suggest that current deformation on the SVF and, at least during the last 5 Ma, is accommodated along its northern and southern terminations where we see a conjunction of young AHe (this study; Bense et al., 2013), bracketed seismicity (Venerdini, 2014) and neotectonic features affecting Quaternary piedmonts (Perucca and Vargas, 2014) in both sectors.

7. Conclusions

We present in this work low thermochronological dating from northern SVF that allows us to complete AHe dataset for this western Pampean range. Comparison with existing data enabled us to constrain the tectonic evolution of this region within the Sierras Pampeanas of west-central Argentina. We obtained Pliocene AHe ages providing evidence for the influence of Neogene exhumation

of the region at about 5 Ma. This might be related to migration of the deformation during the slab flattening of Nazca Plate beneath South America. We note that Permian through Cretaceous AHe ages in the central region of SVF (Coughlin et al., 1998; Bense et al., 2013) could represent either a protracted cooling and limited exhumation (less of 1–3 km) in the last 20 Myr or that the central part of the range may have had existing topographic relief prior to reverse faulting and flat slab subduction of the Nazca plate during the Andean orogeny. The northern region of the SVF, in contrast, shows young AHe (this study and Fosdick et al., 2015), as well as young AFT ages. Assuming a geothermal gradient of 20 °C/km, the Partial Annealing Zone for this last technique is located ~3–4 km bellow surface. Thus, this would suggest that Andean tectonic exhumed at least 3–4 km of rock at the northern SVF during the last 5–6 Ma.

In a regional context, our results suggest an eastward migration of exhumation and agree with the hypothesis of an original single foreland Bermejo basin that was later divided into two (Bermejo and Ischigualasto-Villa Unión) basins on this northern area by exhumation and uplift of the SVF around 3.8–2.6 Ma (Jordan et al., 1988; Cardozo and Jordan, 2001). Finally, a comparison of our results with geodetic, geophysical and neotectonic observations indicates that both terminations, at the north and south of the Sierra de Valle Fértil, are seismically active in agreement with regions of Pliocene cooling ages. However, further determinations are needed to constrain a more complete thermochronological record of key regions all over the SVF and involving AFT, ZHe and AHe observations before we can assess a pattern of deformation within this Pampean range.

Acknowledgments

This research was supported by the Agencia Nacional de Promoción Científica y Tecnológica of Argentina (PICT2011-160), the Secretaría de Ciencia, Estado, Tecnología e Innovación (SECITI) of San Juan and the U. S. National Science Foundation (grant EAR-1049605). We gratefully acknowledge the analytical support from the laboratory personnel at the Arizona Radiogenic Helium Dating Laboratory at the University of Arizona. Critical reviews from José Mescua, anonymous reviewers and the editor helped to improve this paper.

References

Aceñolaza, G., Toselli, A.J., 1988. El Sistema de Famatina, Argentina: su interpretación como orógeno de margen continental activo. In: V Chilean Geological Congress, 1, pp. 55–67. Chile.

Allmendinger, R.W., Figueroa, D., Snyder, D., Beer, J., Mpodozis, C., Isacks, B., 1990. Foreland shortening and crustal balancing in the Andes at 30°S latitude. Tectonics 9, 789–809.

Allmendinger, R.W., Judge, P.A., 2014. The Argentine Precordillera: A foreland thrust belt proximal to the subducted plate. Geosphere 10 (6), 1203–1218.

Alvarado, P., Beck, S., 2006. Source characterization of the San Juan (Argentina) crustal earthquakes of 15 January 1944 (Mw 7.0) and 11 June 1952 (Mw 6.8). Earth Planet. Sci. Lett. 243, 615–631.

Alvarado, P., Beck, S., Zandt, G., Araujo, M., Triep, E., 2005. Crustal deformation in the south-central Andes backarc terranes as viewed from regional broad-band seismic waveform modeling. Geophys. J. Int. 163, 580–598.

Alvarado, P., Pardo, M., Gilbert, H., Miranda, S., Anderson, M., Saez, M., Beck, S., 2009. Flat-slab subduction and crustal models for the seismically active Sierras Pampeanas region of Argentina. In: Kay, S., Ramos, V.A., Dickinson, W. (Eds.), *Backbone of the Americas: Shallow subduction, Plateau uplift, and Ridge and Terrane Collision*, Geol. Soc. Am. Mem., 204, pp. 261–278.

Ammirati, J.B., Alvarado, P., Beck, S., 2015. A lithospheric velocity model for the flat slab region of Argentina from joint inversion of Rayleigh wave phase velocity dispersion and teleseismic receiver functions. Geophys. J. Int. 202, 224–241.

Anderson, M., Alvarado, P., Zandt, G., Beck, S., 2007. Geometry and brittle deformation of the subducting Nazca Plate, Central Chile and Argentina. Geophys. J. Int. 171, 419–434.

Astini, R.A., 2003. The ordovician proto-Andean basins. In: Benedetto, J.L. (Ed.), Ordovician Fossils of Argentina. Secretaría de Ciencia y Tecnología, Universidad Nacional de Córdoba, Córdoba, pp. 1–74.

Bastias, H., 1985. Fallamiento cuaternario en la región sismotectónica de Precordillera, Final Thesis Undergraduate Work in Geology. Universidad Nacional de San Juan, Argentina, p. 185.

Beck, S., Zandt, G., Wallace, T., Anderson, M., Fromm, R., Shearer, T., Wagner, L., Koper, K., Alvarado, P., Triep, E., Lince Klinger, F., Araujo, M., Bufaliza, M., Campos, J., Kausel, E., Ruiz Parades, J., 2001. Charge, the Chile-Argentinean Geophysical Experiment: imaging the south central Andean lithosphere using passive broadband seismology. In: American Geophysical Union, Fall Meeting 2001, Abstract #T31A-0828.

Bense, F.A., Löbens, S., Dunkl, I., Wemmer, K., Siegesmund, S., 2013. Is the exhumation of the Sierras Pampeanas only related to Neogene flat-slab subduction? Implications from a multi-thermochronological approach. J. S. Am. Earth Sci. 48, 123–144.

Brooks, B.A., Bevis, M., Smalley, R.J., Kendrick, E., Manceda, R., Lauría, E., Maturana, R., Araujo, M., 2003. Crustal motion in the Southern Andes (26°–36°S): do the Andes behave like a microplate? Geochem. Geophys. Geosystems 4, 1–14.

Caminos, R., 1979. Cordillera Frontal. In: Castellanos, T.G., Sersic, J.L., Amuchastegui, S., Caputto, R., Cocucci, A.E., Fuchs, G.L., Gordillo, C.E., Melo, C.R. (Eds.), *2do. Simposio de Geología Regional Argentina*, 1. Academia Nacional de Ciencias, Córdoba, Argentina, pp. 394–453.

Cardozo, N., Jordan, T., 2001. Causes of spatially variable tectonic subsidence in the Miocene Bermejo foreland basin, Argentina. Basin Res. 13, 335–357.

Castro de Machuca, B., Arancibia, G., Morata, D., Belmar, M., Previley, L., Pontoriero, S., 2008. P-T-t evolution of an Early Silurian medium-grade shear zone on the west side of the Famatinian magmatic arc, Argentina: implications for the assembly of the Western Gondwana margin. Gondwana Res. 13, 216–226.

Coughlin, T.J., Sullivan, P.B.O., Kohn, B.P., Holcombe, R.J., 1998. Apatite fission-track thermochronology of the Sierras Pampeanas, central western Argentina: Implications for the mechanisms of plateau uplift in the Andes. Geology 26, 999–1002.

Costa, C., Machette, M.N., Dart, R., Bastias, H., Paredes, J., Perucca, L., Tello, G., Haller, K., 2000. Map and Database of Quaternary Faults and Folds in Argentina. USGS, Open-File Report 00–0108.

Criado Roque, P., Mombrú, C., Ramos, V.A., Yrigoyen, M.R., 1981. Estructura e interpretación tectónica. In: VIII Argentinean Geological Congress, San Luis, Argentina, pp. 155–192.

Crowley, P., Reiners, P., Reuter, J., Kaye, G., 2002. Laramide exhumation of the bighorn mountains, Wyoming: an apatite (U-Th)/He thermochronology study. Geology 30, 27–30.

Dávila, F.M., Carter, A., 2013. Exhumation history of the Andean broken foreland revisited. Geology 41 (4), 443–446.

Farley, K.A., 2000. Helium diffusion from apatite; general behavior as illustrated by Durango fluorapatite. J. Geophys. Res. 105, 2903–2914.

Farley, K.A., 2002. (U-Th)/He dating: techniques, calibrations, and applications. In: Porcelli, P.D., Ballestine, C.J., Wieler, R. (Eds.), *Noble Gas Geochemistry*, Rev. Mineral. Geochem., 47, pp. 819–844.

Farley, K.A., Wolf, R.A., 1996. The effects of long alpha-stopping distances on (Ue Th)/He ages. Geochim. Cosmochim. Acta 60 (21), 4223–4229.

Flowers, R.M., Ketcham, R.A., Shuster, D.L., Farley, K.A., 2009. Apatite (U–Th)/He thermochronometry using a radiation damage accumulation and annealing model. Geochim. Cosmochim. Acta 73 (8), 2347–2365. http://dx.doi.org/10.1016/j.gca.2009.01.015.

Fosdick, J.C., Carrapa, B., Ortiz, G., Alvarado, P., 2015. Diachronous faulting and erosion in the Argentine Precordillera: reconciling bedrock cooling and basin provenance records of deformation during changes in subduction regime. Earth Planet. Sci. Lett. (accepted for publication).

Fosdick, J.C., Carrapa, B., 2012. Paleogene initiation of Andean foreland sedimentation in the Bermejo basin and Precordillera thrust belt of NW Argentina from detrital geochronology and thermochronology: geological Society of America. Abstr. Progr. 44 (7), 72.

Gallardo, G., 2011. Determinación de la estructura de velocidades sísmicas a partir de la función del receptor en el flanco oriental de las Sierras de Valle Fértil–La Huerta. Final Thesis Undergraduate Work in Geophysics. Universidad Nacional de San Juan, Argentina, p. 86.

Gans, C.R., Beck, S.L., Zandt, G., Gilbert, H., Alvarado, P., Anderson, M., Linkimer, L., 2011. Continental and oceanic crustal structure of the Pampean flat slab region, western Argentina, using receiver function analysis: new high-resolution results. Geophys. J. Int. 186, 45–58. http://dx.doi.org/10.1111/j.1365-246X.2011.05023.x.

González Bonorino, F., 1950. Algunos problemas geológicos de las Sierras Pampeanas. Rev. Asoc. Geol. Argent. 5, 81–110.

Gordillo, C.E., Lencinas, A., 1981. Geocronología y petrografía de las vulcanitas terciarias del Departamento de Pocho. Provincia de Córdoba. Rev. Asoc. Geol. Argent. 36, 380–388.

INPRES, 2015. Instituto Nacional de Prevención Sísmica, Argentina. Earthquake catalog. www.inpres.gov.ar.

Introcaso, A., Pacino, M.C., Fraga, H., 1992. Gravity, isostasy and Andean crustal shortening between latitudes 30 and 35°S. Tectonophysics 205, 31–48.

Johnson, N.M., Jordan, T.E., Johnson, P.A., Naeser, C.W., 1986. Magnetic polarity stratigraphy, age and tectonic setting of fluvial sediments in an eastern Andean foreland basin, San Juan Province, Argentina. In: Allen, P., Homewood, P. (Eds.), Foreland Basins: International Association of Sedimentologists, vol. 8. Special Publication, pp. 63–75.

Jordan, T., Flemings, P.B., Beer, J.A., 1988. Dating of thrust fault activity by use of foreland-basin strata. In: Kleinspehn, K., Paola, C. (Eds.), New perspectives in basin analysis. Springer-Verlag, New York, pp. 307–330.
Jordan, T.E., Isacks, B., Ramos, V.A., Allmendinger, R.W., 1983a. Mountain building in the Central Andes. Episodes 3, 20–26 (Ottawa, USA).
Jordan, T.E., Isacks, B.L., Allmendinger, R.W., Brewer, J.A., Ramos, V.A., Ando, C.J., 1983b. Andean tectonics related to geometry of subducted Nazca plate. Geol. Soc. Am. Bull. 94, 341–361.
Jordan, T., Allmendinger, R., 1986. The Sierras Pampeanas of Argentina: a modern analogue of Laramide deformation. Am. J. Sci. 286, 737–764.
Jordan, T.E., Allmendinger, R.W., Damanti, J.F., Drake, R., 1993. Chronology of motion in a complete thrust belt: the Precordillera, 30–31°S, Andes Mountains. J. Geol. 101, 135–156. http://dx.doi.org/10.1086/648213.
Jordan, T.E., Schlunegger, F., Cardozo, N., 2001. Unsteady and spatially variable evolution of the Neogene Andean Bermejo foreland basin, Argentina. J. S. Am. Earth Sci. 14, 775–798. http://dx.doi.org/10.1016/S0895-9811(01)00072-4.
Kadinsky-Cade, K., Reilinger, R., Isacks, B., 1985. Surface deformations associated with the November 23, 1977, Caucete, Argentina, earthquake sequence. J. Geophys. Res. 90, 12691–12700.
Kay, S.M., Abbruzzi, J.M., 1996. Magmatic evidence for Neogene lithospheric evolution of the central Andean "flat-slab" between 30°S and 32°S. Tectonophysics 259, 15–28.
Kay, S.M., Gordillo, E., 1994. Pocho volcanic rocks and the melting of depleted continental lithosphere above a shallowly dipping subduction zone in the Central Andes. Contrib. Mineral. Petrol. 117, 25–44.
Kay, S.M., Mpodozis, C., 2002. Magmatism as a probe to the Neogene shallowing of the Nazca plate beneath the modern Chilean fl at-slab. J. S. Am. Earth Sci. 15, 39–57. http://dx.doi.org/10.1016/S0895-9811(02)00005-6.
Kay, S.M., Mpodozis, C., Ramos, V.A., Munizaga, F., 1991. Magma source variations for mid-late Tertiary magmatic rocks associated with a shallowing subduction zone and thickening crust in the Central Andes (28°–33°S). Geol. Soc. Am. Spec. Paper 26, 113–137.
Ketcham, R.A., 2005. Forward and inverse modeling of low-temperature thermochronometry data. Rev. Mineral. Geochem. 58, 275–314.
Langer, C.J., Bollinger, G.A., 1988. Aftershocks of the western Argentina (Caucete) earthquake of 23 November 1977: some tectonic implications. Tectonophysics 148, 131–146.
Langer, C.J., Hartzell, S., 1996. Rupture distribution of the 1977 western Argentina earthquake. Phys. Earth Planet. Interiors 94, 121–132.
Lince, F., Gimenez, M., Martinez, P., Introcaso, A., 2008. Las estructuras de la cuenca de Bermejo y Sierra de Valle Fértil a partir de los métodos Deconvolución de Euler y Señal Analítica. Rev. la Asoc. Geol. Argent. 63, 281–287.
Llambias, E.J., Brogioni, N., 1981. Magmatismo Mesozoico y Cenozoico. In: Geología de La Provincia de San Luis. VIII Argentinean Geological Congress. Relatorio, San Luis, pp. 101–115.
Löbens, S., Bense, F.A., Wemmer, K., Dunkl, I., Costa, C.H., Layer, P., Siegesmund, S., 2011. Exhumation and uplift of the Sierras Pampeanas: preliminary implications from KeAr fault gouge dating and low-T thermochronology in the Sierra de Comechingones (Argentina). Int. J. Earth Sci. 100 (2–3), 671–694.
Löbens, S., Sobel, E.R., Bense, F.A., Wemmer, K., Dunkl, I., Siegesmund, S., 2013. Refined thermochronological aspects of the Northern Sierras Pampeanas. Tectonics 32 (3), 453–472.
Losada-Calderón, A., McBride, S., Bloom, M., 1994. The geology and 40Ar/39Ar geochronology of magmatic activity and related minerlization in the Nevados del Famatina Mining District, La Rioja province, Argentina. J. S. Am. Earth Sci. 7 (1), 9–24.
Malizia, D.C., Reynolds, J.H., Tabbutt, K., 1995. Cronología de la sedimentación Neógena, tectonismo y edad de la estructuración en el Campo de Talampaya, pp. 78–105. Sierras Pampeanas, Provincia de La Rioja, Argentina, YPF, BIP Junio.
McCalpin, J.P., 2009. Paleoseismology, 95. Academic Press, California, USA, p. 629.
Martinez, A., Rodriguez Blanco, L., Ramos, V.A., 2006. Permo-Triassic magmatism of the Choiyoi Group in the Cordillera Frontal of Mendoza, Argentina: geological variations associated with changes in Paleo-Benioff zone. In: Backbone of the Americas Conference. GSA, Mendoza, Argentina, p. 60.
Milana, J.P., Alcober, O., 1994. Modelo tectosedimentario de la cuenca Triásica de Ischigualasto (San Juan, Argentina). Asoc. Geol. Argent. 49 (3–4), 217–235.
Miller, H., Söllner, F., 2005. The Famatinian complex (NW Argentina): back-docking of an island arc or terrane accretion? Early Palaeozoic geodynamics at the western Gondwana margin. In: Terrane Processes at the Margins of Gondwana: Geological Society, vol. 246. Special Publications, London, pp. 241–256.
Monsalvo, V.G., Alvarado, P., Saez, M., Linkimer, L., Bilbao, I., 2014. Deformación sísmica reciente de la sierra de Pie de Palo, Provincia de San Juan. Rev. Asoc. Geol. Argent. 71 (2), 260–266.
Otamendi, J.E., Vujovich, G.I., de la Rosa, J.D., Tibaldi, A.M., Castro, A., Martino, R.D., Pinotti, L.P., 2009. Geology and petrology of a deep crustal zone from the Famatinian paleoarc, Sierras de Valle Fértil and La Huerta, San Juan, Argentina. J. S. Am. Earth Sci. 27, 258–279.
Perucca, L.P., Vargas, N., 2014. Neotectónica de la provincia de San Juan, centro-oeste de Argentina. Bol. Soc. Geol. Mex. 66 (2), 291–304.
Rabassa, J., Carignano, C., Cioccale, M., 2010. Gondwana paleosurfaces in Argentina: an introduction. Geociências 29 (4), 439–466.
Ramos, V.A., 1994. Terranes of southern Gondwanaland and their control in the Andean structure (30-33°S lat.). In: Reutter, K.J., Scheuber, E., Wigger, P.J. (Eds.), Tectonics of the Southern Central Andes, Structure and Evolution of an Active Continental Margin. Springer, Berlin, Germany, pp. 249–261.
Ramos, V.A., 2000. Evolución tectónica de la Argentina. In: Caminos, R. (Ed.), Geología Argentina. Instituto de Geología y Recursos Minerales, Anales, pp. 715–784, 29(24).
Ramos, V., Vujovich, G., 2000. Hoja Geológica San Juan, Escala 1:250.000, Tech. Rep. Servicio GeológicoMinero Argentino Boletín, BuenosAires.
Ramos, V.A., Cristallini, E.O., Pérez, D.J., 2002. The Pampean flat-slab of the central Andes. J. S. Am. Earth Sci. 15 (1), 59–78.
Ramos, V.A., Folguera, A., 2009. Andean Flat-slab Subduction through Time. Geological Society, vol. 327. Special Publications, London, pp. 31–54.
Ramos, V.A., Vujovich, G., Martino, R., Otamendi, J., 2010. Pampia: a large cratonic block missing in the Rodinia supercontinent. J. Geodyn. 50, 243–255.
Rapela, C.W., Pankhurst, R.J., Casquet, C., Fanning, C.M., Baldo, E.G., González-Casado, J.M., Galindo, C., Dahlquist, J., 2007. The Río de la Plata Craton and the assembly of SW Gondwana. Earth Sci. Rev. 83, 49–82.
Reiners, P.W., Spell, T.L., Nicolescu, S., Zanetti, K.A., 2004. Zircon (U-Th)/He thermochronometry: he diffusion and comparisons with 40Ar/39Ar dating. Geochim. Cosmochim. Acta 68, 1857–1887.
Reiners, P.W., Nicolescu, S., 2007. ARHDL Report 1: Measurement, no. December 2006.
Reynolds, J., 1987. Chronology of Neogene Tectonics in the Central Andes (27°-33° S) of Western Argentina Based on the Magnetic Polarity Stratigraphy of Foreland Basin Sediments (Ph.D. Dissertation). Dartmouth College, New Hampshire, USA, p. 353 (unpublished).
Rosello, E., Mozetic, M., Cobbold, P., Urreiztieta, Marc de, Gapais, D., López-Gamundí, O., 1996. The Valle Fértil flower structure and its relationship with the Precordillera and Pampean Ranges (30-32ºS, Argentina). Third ISAG 9, 481–484.
Rosello, E., Mozetic, M.E., 1999. Caracterización estructural y significado geotectónico de los depocentros cretácicos continentales del centro-oeste Argentino. In: 5° Simposio sobre o Cretáceo do Brasil, Serra Negra. Boletín, pp. 107–113.
Rothis, M., Santi Malnis, P., Pantano, A., Perucca, L., 2012. Evidencias de reactivación cuaternaria de la falla maestra de la cuenca triásica de Marayes, al norte del cerro Pan de Azúcar, Sierras Pampeanas occidentales, San Juan, Argentina. In: XV Reunión de Tectónica y IV Reunión de Campo. San Juan. Argentina, p. 131.
Siame, L.L., Bellier, O., Sébrier, M., Araujo, M., 2005. Deformation partitioning in flat subduction setting: case of the Andean foreland of western Argentina (28°S–33°S). Tectonics 24 (5), 1–24. http://dx.doi.org/10.1029/2005TC001787.
Siame, L., Sébrier, M., Bellier, O., Bourlès, D., Costa, C., Ahumada, E., Gardini, C., Cisneros, H., 2015. Active basement uplift of Sierra Pie de Palo (Northwestern Argentina): Rates and inception from ^{10}Be cosmogenic nuclide concentratios. Tectonics 34 (6), 1129–1153.
Snyder, D.B., Ramos, V.A., Allmendinger, R.W., 1990. Thick-skinned deformation observed on deep seismic reflection profiles in Western Argentina. Tectonics 9, 773–788.
Spalletti, L.A., 1999. Cuencas triásicas del Oeste argentino: origen y evolución. Acta Geol. Hispánica 32, 29–50.
Steenken, A., López de Luchi, M.G., Siegesmund, S., Wemmer, K., Pawlig, S., 2004. Crustal provenance and cooling of the basement complexes of the Sierra de San Luis: an insight into the tectonic history of the proto-Andean margin of Gondwana. Gondwana Res. 7 (4), 1171–1195.
Strecker, M.R., 1987. Late Cenozoic Landscape Development, the Santa María Valley, Northewest Argentina (PhD. Thesis). Cornell University, Ithaca, N.Y. USA, pp. 1–262.
Strecker, M., Cerveny, P., Bloom, A., Malizia, D., 1989. Late Cenozoic tectonism and landscape development in the foreland of the Andes: Northern Sierras Pampeanas (26°–28°S), 8. Tectonics, Argentina, pp. 517–534.
Tosselli, A., 1996. In: Andino, Volcanismo, Aceñolaza, F.G., Miller, H., Toselli, A.J. (Eds.), Geología del Sistema de Famatina. Münchner Geologische Heste, Germany, p. A25.
Tripaldi, A., Net, L., Limarino, L., Marenssi, S., Re, G., Caselli, A., 2011. Paleoambientes sedimentarios y procedencia de la Formación Vinchina, Mioceno, noroeste de la prov. de La Rioja. Rev. Asoc. Geol. Argent. 56 (4), 443–465.
Uliana, M.A., Biddle, K.T., Cerdan, J., 1989. Mesozoic extension and the formation of Argentine sedimentary basins. AAPG Mem. 46, 599–614.
Venerdini, A., 2014. Modelo cortical de velocidades sísmicas para la región comprendida entre 30,0°S – 32,5°S y 67,0°O – 68,5°O, p. 110. Final Thesis Undergraduate Work in Geophysics Universidad Nacional de San Juan, Argentina.
Vujovich, G., van Staal, C., Davis, W., 2004. Age constrains on the tectonic evolution and provenance of the Pie de Palo Complex, Cuyania composite terrane, and the Famatinian orogeny in the Sierra de Pie de Palo, San Juan, Argentina. Gondwana Res. 7 (4), 1041–1056.
Wolf, R.A., Farley, K.A., Silver, L.T., 1996. Helium diffusion and low-temperature thermochronometry of apatite. Geochim. Cosmochim. Acta 60 (21), 4231–4240.
Wolf, R.A., Farley, K.A., Kass, D.M., 1998. Modeling of the temperature sensitivity of the apatite (U-Th)/He thermochronometer. Chem. Geol. 148 (1-2), 105–114.
Yañez, G., Ranero, G.R., Huene, R., von Díaz, J., 2001. Magnetic anomaly interpretation across a segment of the Southern Central Andes (32–34°S): implications on the role of the Juan Fernández Ridge in the tectonic evolution of the margin during upper Tertiary. J. Geophys. Res. 106, 6325–6345.
Zapata, 1998. Crustal structure of the Andean thrust front at 30 degrees S latitude from shallow and deep seismic reflection profiles, Argentina. J. S. Am. Earth Sci. 11, 131–151.
Zapata, T.R., Allmendinger, R.W., 1996. Thrust front zone of the Precordillera, Argentina: a thick-skinned triangle zone. Am. Assoc. Petroleum Geol. Bull. 80, 359–381.
Zeitler, P.K., Herczeg, A.L., McDougall, I., Honda, M., 1987. U-Th-He dating of apatite: a potential thermochronometer. Geochim. Cosmochim. Acta 51, 2865–2868.